Journal of Solid State Chemistry **160,** 17–24 (2001)
doi:10.1006/jssc.2001.9119, available online at http://www.idealibrary.com on IDEAL®

Ab Initio Structure Solution of $BaFeO_{2.8-\delta}$, a New Polytype in the System $BaFeO_y$ ($2.5 \leq y \leq 3.0$) Prepared from the Oxidative Thermal Decomposition of $BaFe[(CN)_5NO] \cdot 3H_2O$

María Inés Gómez, Gabriela Lucotti, and Juana A. de Morán

Instituto de Química Inorgánica, Facultad de Bioquímica, Química y Farmacia, Universidad Nacional de Tucumán, Ayacucho 491, 4000 San Miguel de Tucumán, Argentina

Pedro J. Aymonino[1]

CEQUINOR (CONICET, UNLP) and LANAIS EFO (CONICET, UNLP), Departamento de Química, Facultad de Ciencias Exactas, Universidad Nacional de La Plata, CC 962, 1900 La Plata, Argentina

Silvina Pagola[2] and Peter Stephens

Department of Physics and Astronomy, State University of New York at Stony Brook, Stony Brook, New York 11794-3800, USA

and

Raúl E. Carbonio[1,3]

Instituto de Investigaciones en Físico Química de Córdoba (INFIQC), Departamento de Físico Química, Facultad de Ciencias Químicas, Universidad Nacional de Córdoba, Ciudad Universitaria, 5000 Córdoba, Argentina

Received October 4, 2000; in revised form January 17, 2001; accepted February 9, 2001; published online June 7, 2001

$BaFeO_{2.8-\delta}$ with a crystal structure different from any of those previously reported in the system $BaFeO_y$ ($2.5 \leq y \leq 3.0$) was prepared by a low-temperature method of synthesis, based on the oxidative thermal decomposition of $BaFe[(CN)_5NO] \cdot 3H_2O$. The structure was solved ab initio by high-resolution synchrotron X-ray powder diffraction and refined by Rietveld analysis ($R_P = 7.78$, $R_{wp} = 11.3$, $R_{exp} = 3.76$, $R_{Bragg} = 6.67$, $\chi^2 = 9.03$). The compound crystallizes in the hexagonal crystal system, space group $P6_3/mmc$, $Z = 10$, unit cell parameters $a = 5.77944(1)$, $c = 24.60871(6)$ Å. The structure consists of 10H close packed $(hchch)_2$ stacking of BaO_n layers (eight BaO_3 layers and two oxygen-deficient BaO_2 layers). Additional oxygen deficiencies are randomly distributed on the h BaO_3 layers. Six iron ions occupy octahedral sites sharing faces between them along the c axis and four occupy tetrahedral sites (2 T^+ and 2 T^-) sharing faces with the octahedra and sharing corners between them.

Key Words: **$BaFeO_{2.8-\delta}$; ab initio structure solution; new polytype; synchrotron X-ray diffraction.**

INTRODUCTION

ABO_y perovskite type oxides ($2.5 \leq y \leq 3.0$, A = lanthanide or alkaline earth, B = transition metal) have great technological interest due to their electrical, magnetic, and catalytic properties (1). They have been extensively used as catalysts in redox reactions, as the reduction of nitrogen oxides and SO_2 (2, 3), hydrogenation of hydrocarbons (4), oxidation of carbon monoxide and ammonia (5), and in the elimination of atmospheric pollution (6). For the specific case of $AFeO_y$, iron can be in oxidation states $3+$ or $4+$. During the synthesis of compounds in this system, a large number of oxygen vacancies are usually generated (7–11) due to the high instability of Fe^{4+}, and in the extreme case, a brownmillerite type compound is formed with all the iron in oxidation state $3+$ (8). The generation of oxygen vacancies is increased as the synthesis temperature increases. Temperatures as high as 1400°C are used in order to produce well defined structures. In such cases, oxygenation at lower temperatures is needed to decrease the number of

[1] Members of the Research Career of the National Scientific and Technological Research Council of Argentina.

[2] Permanent address: Instituto de Investigaciones en Físico Química de Córdoba (INFIQC), Departamento de Físico Química, Facultad de Ciencias Químicas, Universidad Nacional de Córdoba, Ciudad Universitaria, 5000 Córdoba, Argentina.

[3] To whom correspondence should be addressed.

0022-4596/01 $35.00

oxygen vacancies. Moreover, for catalytic purposes, low temperatures are needed in order to produce high surface area catalysts with a high content of Fe^{4+} (12). For these reasons, the search for a low temperature synthetic method is crucial in these systems. The thermal decomposition of inorganic complex salts with the metals in the desired ratio is usually a good method of producing mixed oxides at low temperatures (6, 13–16).

The first detailed determination of cell parameters for several phases in the system $BaFeO_y$ ($2.5 \leq y \leq 3.0$) has been informed by Mori (11). A hexagonal phase was found for compositions in the range $BaFeO_{2.63-2.92}$ with a wide range in oxygen contents; the other phases have limited compositions: the triclinic I, $BeFeO_{2.50}$; triclinic II, $BaFeO_{2.64-2.67}$, rombohedral I and II, $BaFeO_{2.62-2.64}$; and tetragonal, $BaFeO_{2.75-2.81}$. Several detailed structural determinations have been reported (17–24) using X-rays and/or neutron and/or electrons diffraction, for some of the compounds in this system.

In the present work we report a new polytype in the system $BaFeO_y$ ($2.5 \leq y \leq 3.0$), which has been prepared by the low-temperature thermal decomposition of barium nitroprusside. The structure has been solved ab initio from synchrotron powder X-ray diffraction.

EXPERIMENTAL

$Ba[Fe(CN)_5NO]\cdot 3H_2O$ was prepared by the indirect method from silver nitroprusside, as it cannot be obtained directly from sodium nitroprusside (25).

The double decomposition reactions are

$$[Fe(CN)_5NO]^{2-}_{(aq)} + 2\ Ag^{+}_{(aq)} \rightarrow Ag_2[Fe(CN)_5NO]_{(s)}$$

$$Ag_2[Fe(CN)_5NO]_{(s)} + Ba^{2+}_{(aq)} + 2\ Cl^{-}_{(ac)} \rightarrow Ba^{2+}_{(aq)} + [Fe(CN)_5NO]^{2-}_{(aq)} + 2AgCl_{(s)}.$$

The obtained solution was separated from the solid by centrifugation and concentrated by evaporation. Barium nitroprusside was obtained as a reddish crystalline compound and its trihydrate was stabilized in a drier under $CaCl_2$. The sample showed red grayish acicular crystals, very soluble in water. Barium nitroprusside salts mono-, di-, tri-, and hexahydrates were reported previously by other authors (26–28).

$BaFeO_{2.8-\delta}$ samples were obtained by oxidative thermal decomposition of $Ba[Fe(CN)_5NO]\cdot 3H_2O$, following the procedure described in a previous publication (16). In the present case the sample used for the structural refinement was prepared as follows: a sample of $Ba[Fe(CN)_5NO]\cdot 3H_2O$ was heat treated under O_2 atmosphere at 850°C for 12 h, five times with intermediate grindings. The decomposition process was followed using samples prepared at different temperatures and times under oxygen atmosphere.

The Giles and Trivedi technique (29) was used in order to determine surface areas. This method has proved to be useful for many inorganic solids (16, 30, 31). Methylene blue was used as adsorbate. Even if dye adsorption in solution might have the problem of pore accessibility by the dye molecule, surface areas obtained in the present work are in the order of areas reported for nonporous materials, in which case this method reproduced BET measurements (30).

Infrared spectroscopy (IRS), powder X-ray diffraction (XRD), and thermogravimetric analysis (TGA) were used in order to follow the decomposition process. IR spectra were recorded with FTIR Perkin Elmer 1600 and Brucker IFS 66 spectrophotometers. XRD data were recorded using a Rigaku Miniflex diffractometer Model CN 2005. Scanning electron microscopy (SEM) photographs were taken with a JOEL JSM 35CF.

The high-resolution room temperature X-ray powder diffraction pattern for the structural analysis was collected at the SUNY X3B1 powder diffraction beamline, NSLS, Brookhaven National Laboratory. The wavelength (0.699852 Å) was selected by a monochromator consisting of two parallel Si(111) crystals. The incident beam was monitored by an ion chamber. The out-of-plane resolution in the diffracted beam was given by slits whereas the in-plane resolution was determined by a Ge(111) analyzer crystal. The diffracted beam was measured with a NaI(Tl) scintillation detector. The sample was rocked about the diving portion in a zero-background quartz sample holder. Data were collected in the range $2^\circ \leq 2\theta \leq 48^\circ$ with a step size of 0.005° and a counting time of 3.5 s per step.

The EXPO program (32) was used to solve the structure by direct methods. A Le Bail profile fit (33) was done using the program FULLPROF (34), a strongly modified version of the Young and Wiles refinement program (35). A pseudo-Voigt function convoluted with an axial divergence asymmetry function (36) was chosen to generate the line shapes. The background intensities were subtracted as the linear interpolation between 97 given points. No regions were excluded and the following parameters were refined: zero-point, pseudo-Voigt parameters of the peak shape, full width at half maximum, and cell parameters.

The structural refinement was performed by the Rietveld method (37), using the FULLPROF program (34). Since a small amount of $BaCO_3$ was detected in the patterns, its structural model (38) was included in the refinement. During the Rietveld refinement the profile parameters were fixed at the values obtained in the Le Bail profile fit. In the final runs the following parameters were refined: scale factors, positional parameters and thermal isotropic parameters. The thermal isotropic parameters of all the oxygens were refined at the same value. After the refinement converged, the isotropic thermal parameters for the oxygens were kept constant and the O occupancies were refined constrained to their maximum allowed values. In the final refinement

cycles, the shifts in the atomic parameters were zero up to the fourth decimal figure.

RESULTS AND DISCUSSION

In Fig. 1 we show the percentage of residual weight of samples of $Ba[Fe(CN)_5NO]\cdot 3H_2O$ heat treated in the furnace under air atmosphere, as a function of temperature. It is clear from the figure that the decomposition process follows three steps. The first one is due to the loss of three water molecules. In the second step, NO and one CN group evolve and in the last step the evolution of the remaining CN groups takes place together with the takeup of oxygen to form the oxide. The total weight loss ends at ca. 820°C. The final residual weight value is in agreement with the theoretical value predicted, which should be between 57.25 and 59.21% for $BaFeO_{2.5}$ and $BaFeO_3$, respectively, as final products.

The reactions taking place during the decomposition process can be represented by the following equations:

$$Ba[Fe(CN)_5NO]\cdot 3H_2O \rightarrow Ba[Fe(CN)_5NO] + 3H_2O \text{ (Step 1)}$$

$$Ba[Fe(CN)_5NO] \rightarrow \tfrac{1}{2}\, BaFe[Fe(CN)_6] + \tfrac{1}{2}\, Ba(CN)_2 + \tfrac{1}{2}\, C_2N_2 + NO \text{ (Step 2)}$$

$$\tfrac{1}{2}\, BaFe[Fe(CN)_6] + \tfrac{1}{2}\, Ba(CN)_2 + 5O_2 \rightarrow \tfrac{1}{2}\, BaCO_3 + \tfrac{1}{2}\, BaO + FeO + 7/2\, CO_2 + 2N_2 \text{ (Step 3a)}$$

$$\tfrac{1}{2}\, BaFe[Fe(CN)_6] + \tfrac{1}{2}\, Ba(CN)_2 + (8+y)/2\, O_2 \rightarrow BaFeO_y + 4CO_2 + 2N_2 \text{ (Step 3b).}$$

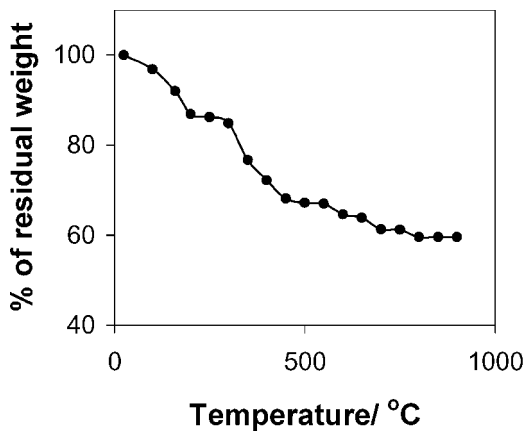

FIG. 1. Dependence of percentage of residual weight as function of temperature for $BaFe[(CN)_5NO]\cdot 3H_2O$ heat treated in the furnace under air atmosphere.

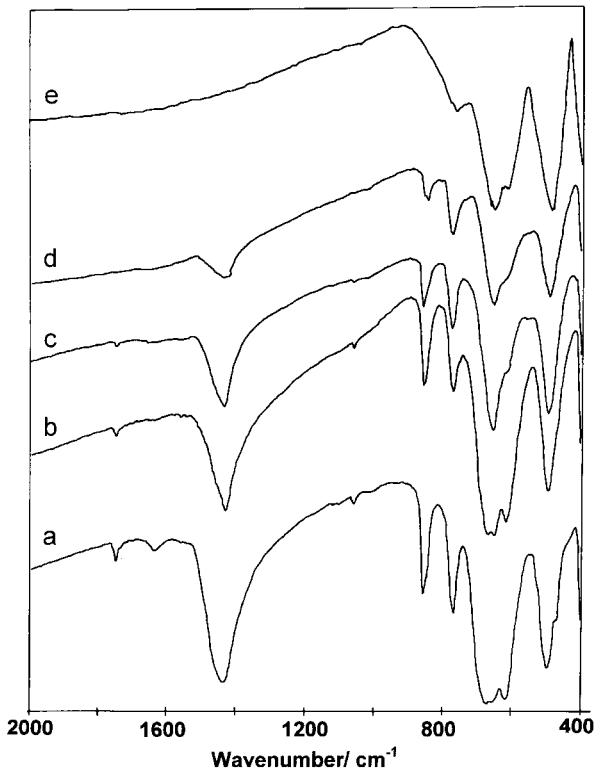

FIG. 2. IR Spectroscopy of samples of $BaFe[(CN)_5NO]\cdot 3H_2O$ heat treated at 850°C during different times: (a) 12 h; (b) 24 h; (c) 36 h; (d) 48 h; (e) 60 h.

Step 3 can proceed either through reactions 3a or 3b depending on the temperature and heating time. The longer the reaction goes through reaction 3b, the higher will be the purity of the sample.

Based on these results, for subsequent studies, samples were heat treated at final temperatures higher than 800°C.

In Fig. 2 we show IR spectra of samples prepared at 850°C with different heating times. Bands assigned to $BaCO_3$ (39) are observed at 1433, 850, and 690 cm^{-1} due to the stretching of C=O and the angular deformations of the CO_3 moiety, respectively, and at lower frequencies, bands characteristic of perovskite oxides are observed (40). It is clear that after five treatments of 12 h we obtain a sample, which according to IRS is free of carbonate. This time was considerably larger than in the calcium and strontium nitroprusside, where heat treatment times of 36 and 48 h were enough (16). This is reasonable taking into account the larger thermal stability of $BaCO_3$.

This low temperature of synthesis represents a considerable improvement in the preparation of $BaFeO_y$ compared to traditional methods, since they require up to 300 h of thermal treatment and extremely high oxygen pressures (10).

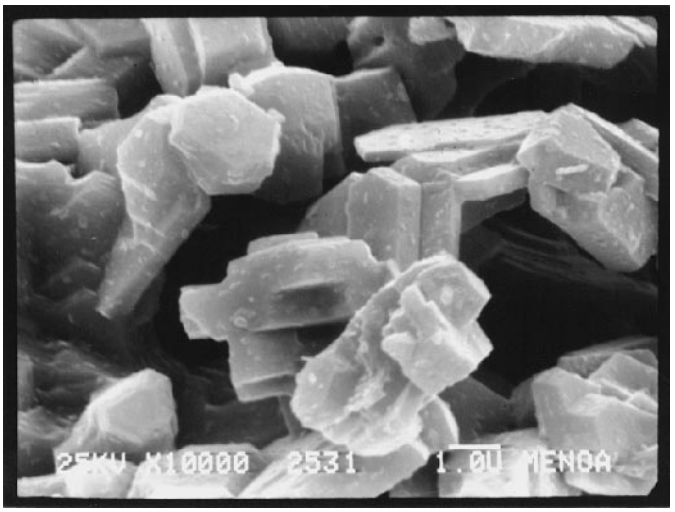

FIG. 3. Scanning electron microscopy of a sample obtained after five heat treatments of 12 h at 850°C under air atmosphere.

TABLE 1

Crystallographic Parameters for $BaFeO_{2.8-\delta}$, after Rietveld Refinement[a] of Synchrotron Powder XRD Data at 298 K (Space Group $P6_3/mmc$ (No. 194)), $Z = 10$, $a = 5.77944(1)$ Å and $c = 24.60871(6)$ Å

Atom	Wyckoff site	x	y	z	B_{iso}	Occ.
Ba1	2*b*	0.00000	0.00000	0.25000	[b]	1
Ba2	4*f*	0.33333	0.66667	0.37222(6)	1.15(3)	1
Ba3	4*f*	0.33333	0.66667	0.96064(6)	0.97(3)	1
Fe1	4*e*	0.00000	0.00000	0.60771(11)	0.93(6)	1
Fe2	4*f*	0.33333	0.66667	0.82184(14)	0.94(6)	1
Fe3	2*a*	0.00000	0.00000	0.00000	1.1(1)	1
O1	12*k*	0.3298(15)	0.1649(15)	0.35075(27)	1.25	1
O2	12*k*	0.7051(14)	0.8525(14)	0.45441(33)	1.25	0.878(6)
O3	2*d*	0.33333	0.66667	0.75000	1.25	1
O4	2*c*	0.33333	0.66667	0.25000	1.25	1

[a] Discrepancy factors: $R_P = 7.78$, $R_{wp} = 11.3$, $R_{exp} = 3.76$, $R_{Bragg} = 6.67$, $\chi^2 = 9.03$.

[b] Anisotropic temperature factors for Ba1: $\beta_{11} = 0.040(1)$, $\beta_{22} = 0.040(1)$, $\beta_{33} = 0.0018(5)$, $\beta_{12} = 0.020(1)$, $\beta_{13} = 0.0$, $\beta_{23} = 0.0$.

Since one of the objectives of this work was to find a low-temperature synthetic method in order to produce high surface area samples with a high Fe^{4+} content useful for catalytic purposes, we used surface area measurements and SEM to characterize the samples.

Surface areas for samples heated between 800 and 900°C were around 2.40 $m^2\ g^{-1}$. These are similar to those found for calcium nitroprusside but lower than for the strontium compound (16). A SEM photograph of the same sample that was used for the structural refinement is shown in Fig. 3. Several well-defined crystals with hexagonal crystalline habits are observed.

Structural Characterization

A comparison with several possible isostructural compounds (41–44) indicated that the cell content should be 10 $BaFeO_y$ and since the exact oxygen content was not known, we tried $Ba_{10}Fe_{10}O_x$ (with $x = 26$, 27, or 28) compositions to run EXPO. The integrated intensities of 297 reflections were used. Only $x = 28$ gave coherent results with a low R value (13.2%). All atoms were unequivocally located in special positions in the space group $P6_3/mmc$. The structural model obtained from EXPO was refined by Rietveld analysis with the FULLPROF program.

The final cell parameters, atomic coordinates, occupancies, thermal isotropic factors (anisotropic for Ba1), and discrepancy factors are shown in Table 1. The excellent agreement between the observed and calculated profiles is shown in Fig. 4. Final selected bonding distances and angles are given in Table 2.

The structure can be described as follows (Fig. 5): a layer (parallel to the *a*–*b* plane) of slightly distorted $(Fe3)(O2)_6$ octahedra share faces with two layers of strongly distorted $(Fe1)(O1)_3(O2)_3$ octahedra. Two layers (parallel to the *a*–*b* plane) of $(Fe2)(O1)_3(O3)$ tetrahedra (one T^+ and one T^-) share common faces with the two layers of strongly distorted $(Fe1)(O1)_3(O2)_3$ octahedra (through common O1) and share corners (through common O3) between them. The average bonding distances (ABD) between iron ions and O^{2-} in these octahedra and tetrahedra (see Table 2) are very close to the sum of ionic radii (SIR) of O^{2-} and the different kinds of iron sites, using the effective ionic radii based on $r(^{VI}O^{2-}) = 1.40$ Å (45). This comparison is shown in Table 3.

The octahedral and tetrahedral interstitial sites occupied by iron ions are generated by a hexagonal close packing framework composed of the stacking of 10 $(Ba^{2+})(O^{2-})_n$ layers which can be described as follows. Ba1 is coordinated to three O3 and three O4 in the same plane ((Ba1)(O3)(O4) oxygen-deficient close packed layer (CPL)) and six O1 (three on top and three at the bottom), with a coordination number (CN) of 12 (Fig. 6a); Ba2 is coordinated to six O1 (out of plane) $((Ba2)(O1)_3$ CPL) and one O4 (at the Ba1(O3)(O4) oxygen-deficient CPL) and three O2 (at the $(Ba3)(O2)_3$ CPL), giving a CN of 10 (Fig. 6b); finally, Ba3 is coordinated to six O2 in the same plane $((Ba3)(O2)_3$ CPL), three O1 (at the $(Ba2)(O1)_3$ CPL), and three O2 at the neighboring $(Ba3)(O2)_3$ CPL, giving a CN of 12 (Fig. 6c). All these Ba^{2+}–O^{2-} ABD (Table 2) are very close to the SIR of $^{XII}Ba^{2+}$ and O^{2-} (3.03 Å).

The long bonding distance (Ba1)–(O3) (3.337 Å) arising from the tetrahedral coordination of Fe2 (notice the short bonding distance (Fe2)–(O3), 1.768 Å) leads to a large

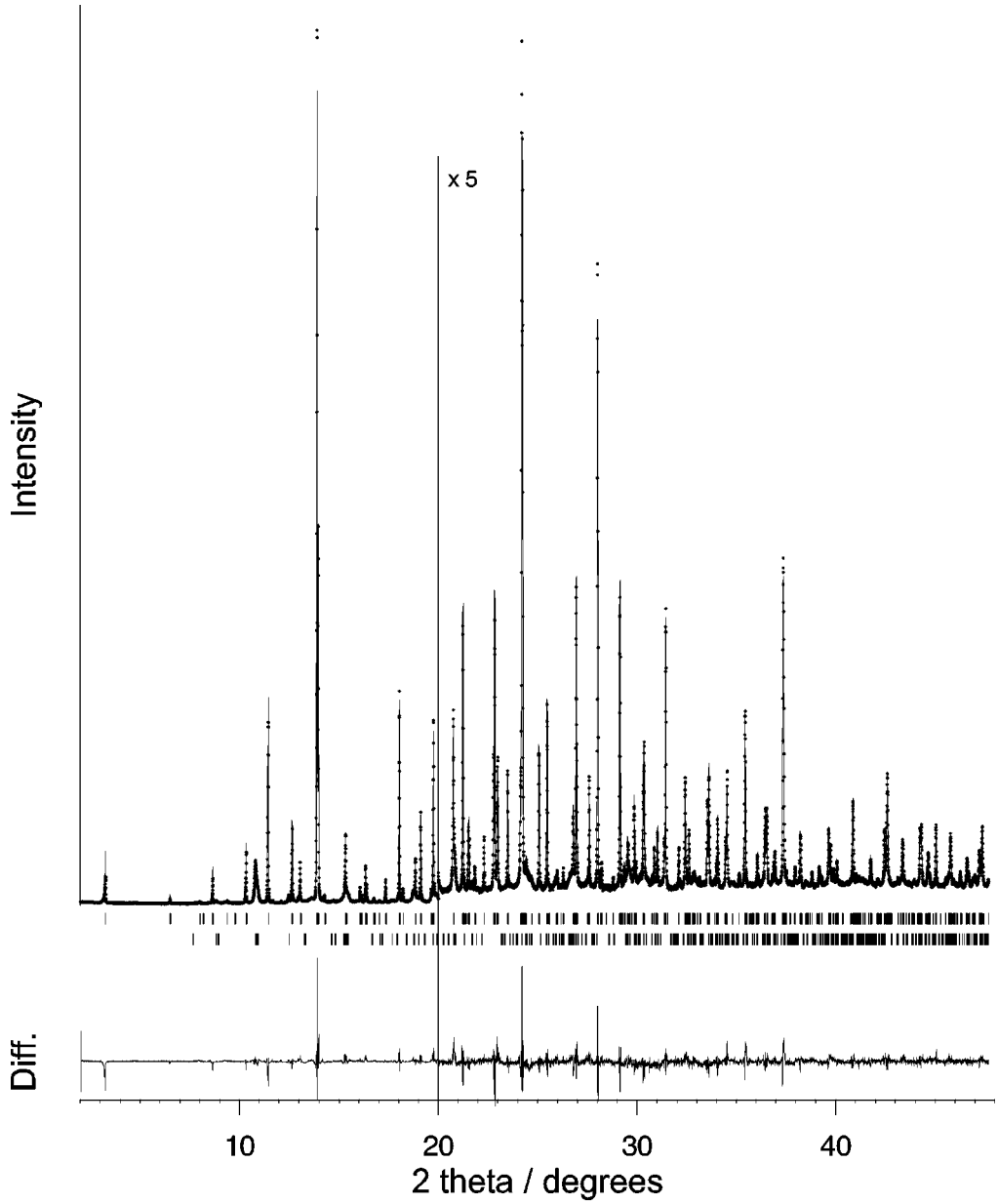

FIG. 4. Observed (crosses), calculated (solid line) and difference (at the bottom) synchrotron X-ray powder diffractogram for $BaFeO_{2.8-\delta}$ synthesized by the oxidative thermal decomposition of $BaFe[(CN)_5NO]\cdot 3H_2O$ at 850°C for 12 h, five times with intermediate grindings under O_2 atmosphere. Zooming ($\times 5$) for $2\theta > 20^\circ$ is shown.

anisotropy of the thermal parameter for Ba1 in the *a–b* plane (see Table 1). The refinement of the anisotropic thermal parameters for the Ba1 resulted in a noticeable decrease of all the *R* values. Similar results were obtained by Shpanchenko *et al.* (44) for $Ba_5Er_2Al_2ZrO_{13}$ and $Ba_{4.5}Sr_{0.5}Sc_{1.33}Al_2Zr_{1.66}O_{13.33}$ even though in this case the layer stacking was different, conducting to a corner sharing of the octahedra but with the same environments for all the barium ions.

The results of the O occupancies refinement show that there are additional O deficiencies, besides those ordered in the *h* (Ba1)(O3)(O4) layers. These vacancies are disordered in the *h* $(Ba3)(O2)_3$ layers and they give rise to a final chemical composition $BaFeO_{2.65(7)}$. In order to confirm this result we performed chemical analyses by iodometric titration for samples prepared at different temperatures. The results are shown in Fig. 7. A comparison of the previous proposed formula with the chemical analysis for the sample

TABLE 2
Some Selected Interatomic Distances (Å) and Bonding Angles (°) for $BaFeO_{2.8-\delta}$

Distances		Angles
$(Ba1)O_{12}$		
(Ba1)–(O1)	2.979(9) × 6	
(Ba1)–(O3)	3.337(0) × 3	
(Ba1)–(O4)	3.337(0) × 3	
⟨(Ba1)–O⟩	3.158(5)	
$(Ba2)O_{10}$		
(Ba2)–(O1)	2.94(1) × 6	
(Ba2)–(O2)	2.742(8) × 3	
(Ba2)–(O4)	3.008(2) × 1	
⟨(Ba2)–O⟩	2.887(3)	
$(Ba3)O_{12}$		
(Ba3)–(O1)	3.19(1) × 3	
(Ba3)–(O2)	2.901(8) × 6	
(Ba3)–(O2)	2.805(9) × 3	
⟨(Ba3)–O⟩	2.947(9)	
$(Fe1)O_6$		$(Fe1)O_6$
(Fe1)–(O1)	1.94(1) × 3	(O1)–(Fe1)–(O1): 95(1)
(Fe1)–(O2)	2.119(9) × 3	(O1)–(Fe1)–(O2): 166(1)
⟨(Fe1)–O⟩	2.030(9)	(O1)–(Fe1)–(O2): 95(1)
		(O2)–(Fe1)–(O2): 74(1)
$(Fe2)O_4$		$(Fe2)O_4$
(Fe2)–(O1)	1.83(1) × 3	(O1)–(Fe2)–(O1): 106(2)
(Fe2)–(O3)	1.768(5) × 1	(O1)–(Fe2)–(O3): 113(1)
⟨(Fe2)–O⟩	1.814(9)	
$(Fe3)O_6$		$(Fe3)O_6$
(Fe3)–(O2)	1.859(8) × 6	(O2)–(Fe3)–(O2): 87(1)
⟨(Fe3)–O⟩	1.859(8)	(O2)–(Fe3)–(O2): 93(1)

Note. Only bonding angles for iron sites are shown.

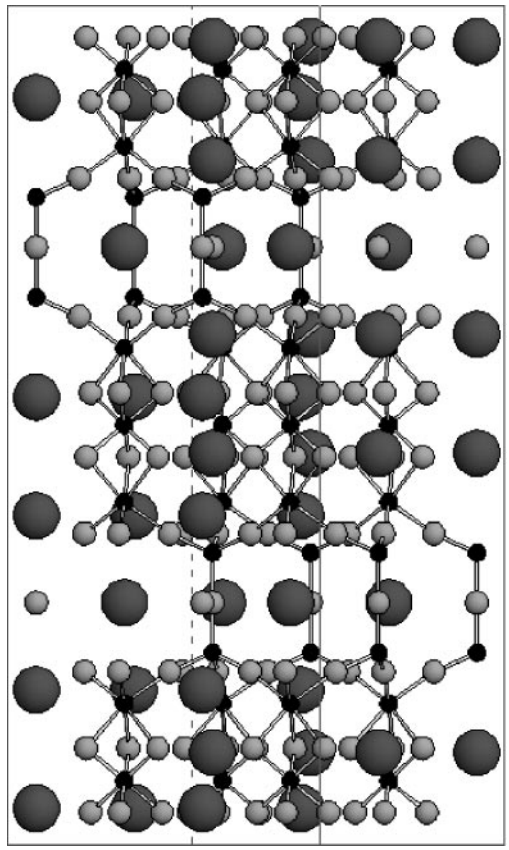

FIG. 5. Projection of the structure of $BaFeO_{2.8-\delta}$ along the [110] direction, showing the linkage of polyhedra around iron sites. Large spheres, barium ions; small black spheres, iron ions; small gray spheres, oxygen ions.

prepared at 850°C shows a very good agreement within the experimental error. Based on the crystalochemical analysis, we propose that there could be a complete range of solid solutions with this structure for compositions between $BaFeO_{2.5}$ and $BaFeO_{2.8}$. The lower limit is established because of the lower possible valence of iron (+3) and the higher limit because of the maximum number of oxygens allowed in this close packed model. Experiments with samples prepared at different temperatures are in progress in order to confirm these assumptions.

In order to get some insight into the distribution of Fe^{3+} and Fe^{4+}, we carried out a series of bond-valence calculations by means of the Brown bond-valence model (46). This model gives a phenomenological relationship between the formal valence of a bond and the corresponding bond lengths. In perfect nonstrained structures, the bond valence sum (BVS) rule states that the valence (V_i) of the cation (anion) is equal to the sum of the bond-valences (v_{ij}) around this cation (anion). The departure from the BVS rule is a measure of the existing stress in the bonds and indicates the presence of covalent bonds. Bond valences are calculated with the formula: $v_{ij} = \exp[(R_{ij} - d_{ij})/0.37]$ (46–48), where R_{ij} is the bond-valence parameter and d_{ij} is the anion–cation distance (in this case the Fe–O^{2-} distance obtained from Table 2). The valence of the atom i (V_i) is then calculated as $\sum_j v_{ij} = V_i$. R_{ij} for the iron–oxygen pair is calculated to be 1.744 according to O'Keeffe and Brese (48). The calculated V_i values are 2.71, 3.31, and 3.86 for Fe(1), Fe(2), and Fe(3), respectively. The large valence exhibited by Fe(3) is due to the extremely short bond length (Fe3)–(O2). This is an indication of a strong covalent bond between an Fe^{4+} and the O^{2-}. These results, together with those shown in Table 3, make Fe(3) the most probable site for Fe^{4+} and Fe(1) and Fe(2) for Fe^{3+}. In order to get concluding results about this distribution, Mössbauer spectroscopy and magnetic susceptibility experiments are in progress and will be presented in another publication.

Despite the limitations of the BVS model and the relatively large errors in the chemical analysis, it is interesting to notice the good agreement between the average oxidation

TABLE 3
Comparison of Average Bonding Distances (ABD) for the Different Polyhedra with the Sum of Ionic Radii (SIR) for the Corresponding Ions

Polyhedron	ABD/Å	Ions[a]	SIR/Å	|ABD-SIR|
$(Fe1)(O1)_3(O2)_3$	2.030(9)	$^{VI}Fe^{3+}_{(HS)}$–O^{2-}	2.045	0.015
		$^{VI}Fe^{4+}$–O^{2-}	1.985	0.045
$(Fe3)(O2)_6$	1.859(8)	$^{VI}Fe^{3+}_{(LS)}$–O^{2-}	1.950	0.091
		$^{VI}Fe^{4+}$–O^{2-}	1.985	0.126
$(Fe2)(O1)_3(O3)$	1.814(9)	$^{IV}Fe^{3+}_{(HS)}$–O^{2-}	1.890	0.076

Note. The absolute value of their differences (|ABD-SIR|) is also shown.
[a] HS, high spin; LS, low spin.

states for iron obtained by these two approaches (3.18 and 3.25, respectively) and the value obtained from the O occupancies refinement (3.30).

CONCLUSIONS

$BaFeO_{2.8-\delta}$ with a crystal structure different from any of those previously reported in the system $BaFeO_y$ ($2.5 \leq y \leq 3.0$) was prepared by a low-temperature method of synthesis, based on the oxidative thermal decomposition of $BaFe[(CN)_5NO]\cdot 3H_2O$. The structure was solved ab initio by high-resolution synchrotron X-ray powder diffraction. The compound crystallizes in space group $P6_3/mmc$, $Z = 10$, unit cell parameters $a = 5.77944(1)$, $c = 24.60871(6)$ Å. The structure consists of 10H close packed $(hchch)_2$ stacking of BaO_n layers (eight BaO_3 layers and two oxygen deficient BaO_2 layers). Additional oxygen deficiencies are randomly distributed on the h BaO_3 layers. Six iron ions occupy octahedral sites sharing faces between them along the c axis and four occupy tetrahedral sites ($2\ T^+$ and $2\ T^-$) sharing faces with the octahedra and sharing corners between them. This new barium ferrate polytype is believed to be stabilized only at this low temperature (850°C) and atmospheric oxygen pressure, since it has not been described for samples prepared with other methods of synthesis. This low temperature of synthesis represents a considerable improvement in the preparation of $BaFeO_y$ compared to traditional methods, since they

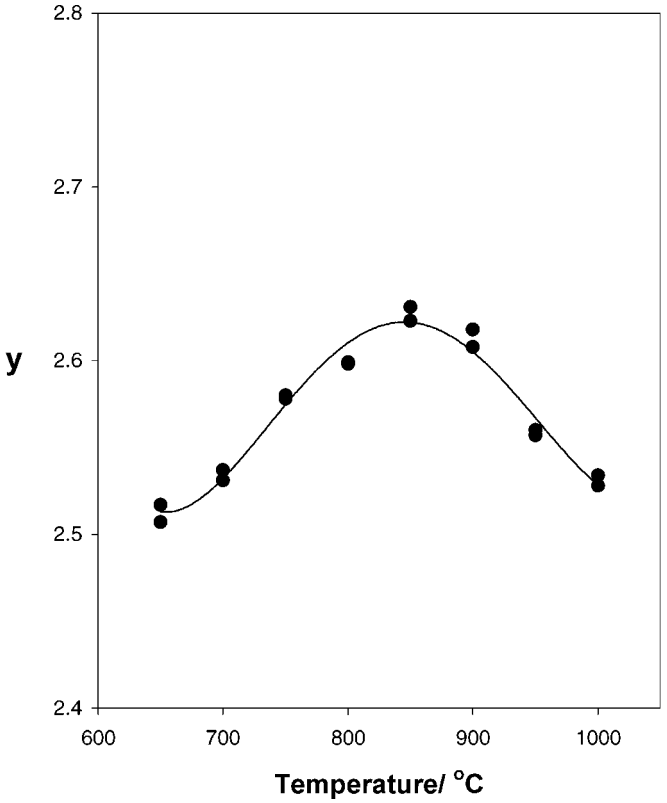

FIG. 7. Oxygen content (y) obtained by iodometric titration for $BaFeO_y$ samples prepared by five heat treatments of 12 h at different temperatures under oxygen atmosphere.

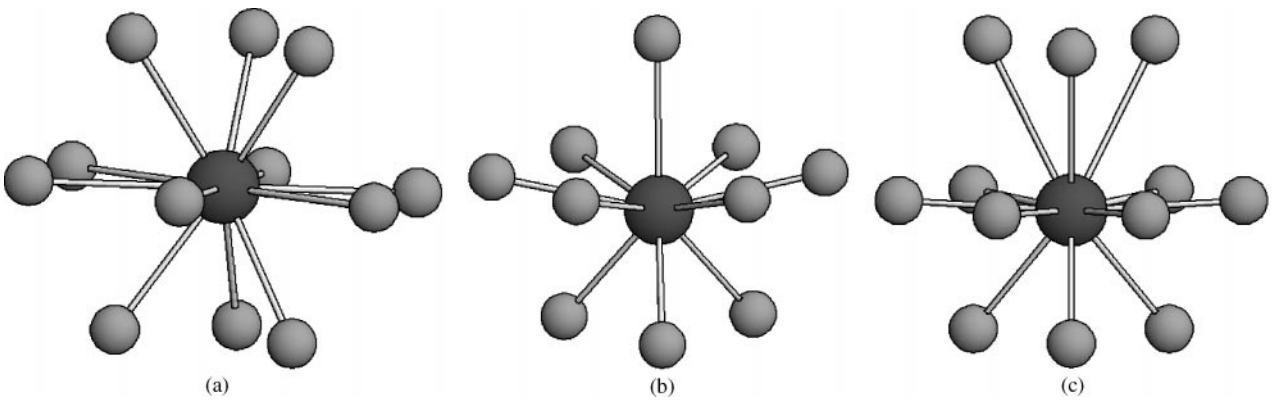

FIG. 6. Oxygen coordination around (a) Ba1, (b) Ba2, and (c) Ba3.

require up to 300 h of thermal treatment and extremely high oxygen pressures. Synthetic methods based on the low temperature oxidative thermal decomposition of inorganic complexes are thus suitable for preparing high-surface-area mixed oxides for catalytic purposes, as well as for preparing new structures not available in the high temperature region.

ACKNOWLEDGMENTS

R.E.C. thanks ANPCYT (Project 06-00062-01128), CONICOR (Project 4582/98), SECYT-UNC (Project 257/98), and CONICET (Project PIP 380/98) for research grants. R.E.C. thanks E. V. Antipov for helpful discussions. R.E.C. and M.I.G. thank Fundación Antorchas for a collaboration project (Project 13740/1-94). P.J.A. thanks CONICET for PIP 4752/96 together with CICPBA for providing financial support to CEQUINOR (CONICET, UNLP). P.J.A. also thanks to ANPCyT for PICT 00118 and to UNLP for an incentive grant. M.I.G. and J.A.de M. thank CIUNT for financial support. Part of this research has been performed at the NSLS, Brookhaven National Laboratory, which is supported by the US DOE, Division of Chemical Sciences and Division of Materials Sciences. Part of this work has been supported by US NSF Grant DMR95-01325. The SUNY X3B1 beamline at the National Synchrotron Light Source is supported by the Division of Basic Energy Sciences of the US DOE (DE-FG02-86ER45231).

REFERENCES

1. L. G. Tejuca and J. L. G. Fierro (Eds.), "Properties and Applications of Perovskite-Type Oxides." Dekker, New York, 1993.
2. R. J. H. Voorhoeve, D. W. Jhonson, Jr., J. P. Remeika, and P. K. Gallagher, *Science* **195,** 827 (1977).
3. D. B. Hibbert and A. C. C. Tseung, *J. Chem. Technol. Biotechnol.* **29,** 713 (1979).
4. J. O. Petunchi, M. A. Ulla, J. I. Nicastro, and E. A. Lombardo, *Seventh Iberoamer. Simp. Catal.* 118 (1980).
5. E. G. Vrieland, *J. Catal.* **32,** 415 (1974).
6. J. M. D. Tascón, S. Mendioroz, and L. Gonzalez Tejuca, *Z. Phys. Chem.* **124,** 109 (1981).
7. Y. Takeda, K. Kanno, T. Takada, O. Yamamoto, M. Takano, N. Nakayama, and Y. Bando, *J. Solid State Chem.* **63,** 237 (1986).
8. P. K. Gallagher, J. B. Mac Chesney, and D. N. E. Buchanan, *J. Chem. Phys.* **41,** 2429 (1964).
9. B. C. Tofield, C. Greaves, and B. E. F. Fender, *Mater. Res. Bull.* **10,** 737 (1975).
10. M. Takano and Y. Takeda, *Bull. Inst. Chem. Res. Kyoto Univ.* **61,** 5 (1983).
11. S. Mori, J. *Am. Chem. Soc.* **49,** 600 (1966).
12. A. G. Andersen, T. Hayakawa, K. Suzuki, M. Shimizu, and K. Takehira, *Catal. Lett.* **27,** 221 (1994).
13. M. Sakamoto, K. Matsuki, R. Ohsumi, Y. Nakayama, Y. Sadaoka, S. Nakayama, N. Matsumoto, and H. Okawa, *J. Chem. Soc. Jpn.* **100,** 1211 (1992).
14. E. Traversa, P. Nunziante, M. Sakamoto, Y. Sadaoka, M. Carotta, and G. Martinelli, *J. Mater. Res.* **13,** 1335 (1998).
15. E. Traversa, M. Sakamoto, and Y. Sadaoka, *Particulate Sci. Tech.* **16,** 185 (1998).
16. M. I. Gómez, J. A. de Morán, R. E. Carbonio, and P. J. Aymonino, *J. Solid State Chem.* **142,** 138 (1999), doi: 10.1006/jssc.1998.8002.
17. X. D. Zou, S. Hovmoeller, M. Parras, J. M. González-Calbet, M. Vallet-Regí, and J. C. Grenier, *Acta Crystallogr. A* **49,** 27 (1993).
18. M. Parras, L. Fournes, J. C. Grenier, M. Pouchard, M. M. Vallet, J. M. Calbet, and P. Hagenmüller, *J. Solid State Chem.* **88,** 261 (1990).
19. J. C. Grenier, L. Fournes, M. Pouchard, P. Hagenmüller, M. Parras, M. Vallet, and J. Calbet, *Z. Anorg. Allg. Chem.* **576,** 108 (1989).
20. J. C. Grenier, A. Wattiaux, M. Pouchard, P. Hagenmüller, M. Parras, M. Vallet, J. Calbet, and M. A. Alario-Franco, *J. Solid State Chem.* **80,** 6 (1989).
21. M. Parras, M. Vallet-Regí, J. M. González-Calbet, M. A. Alario-Franco, J. C. Grenier, and P. Hagenmüller, *Mater. Res. Bull.* **22,** 1413 (1987).
22. A. J. Jacobson, *Acta Crystallogr. B* **32,** 1087 (1976).
23. E. Lucchini, S. Meriani, and D. Minichelli, *Acta Crystallogr. B* **29,** 1217 (1973).
24. M. Zanne and C. Gleitzer, *Bull. Soc. Chim. Fr.* **1971,** 1567 (1971).
25. L. A. Gentil, E. J. Baran, and P. J. Aymonino, *Z. Naturforsch.* **23b,** 1264 (1968).
26. D. V. Parwate and A. Garg, *Int. J. Chem. A* **25,** 151 (1985).
27. M. Chamberlain and A. J. Greene, Jr., *J. Inorg. Nucl. Chem.* **25**(11), 1471 (1963).
28. E. L. Varetti and P. J. Aymonino, *Inorg. Chim. Acta* **7,** 597 (1973).
29. C. H. Giles and A. S. Trivedi, *Chem. Ind.* **40,** 1426 (1969).
30. J. A. de Morán, D. Castillo, A. Benavente, and M. I. G. de Díaz, *Anal. Asoc. Quim. Arg.* **83,** 1–2 (1995).
31. L. A. Sales and J. A. De Morán, *Anal. Asoc. Quim. Arg.* **63,** 251 (1975).
32. A. Altomare, M. C. Burla, B. Carrozzini, G. L. Cascarano, C. Giacovazzo, A. Guagliardi, A. G. G. Moliterni, G. Polidori, and R. Rizzi, *J. Appl. Crystallogr.* **32,** 339 (1999).
33. A. LeBail, H. Duroy, and J. L. Fourquet, *Mater. Res. Bull.* **23,** 447 (1988).
34. J. Rodríguez-Carbajal, *Physica B* **192,** 55 (1993).
35. D. B. Wiles and R. A. Young, *J. Appl. Crystallogr.* **14,** 149 (1981).
36. L. W. Finger, D. E. Cox, and A. P. Jephcoat, *J. Appl. Crystallogr.* **27,** 892, 1994.
37. H. M. Rietveld, *J. Appl. Crystallogr.* **2,** 65 (1969).
38. Inorganic Chemical Structure Database, File 15196.
39. R. T. Conley, "Infrared Spectroscopy." Ed. Alhambra, Madrid, 1979.
40. K. Nakamoto, "Infrared and Raman Spectra of Inorganic and Coordination Compounds." Part A, 5th ed. Wiley, New York, 1997.
41. T. Negas and R. S. Roth, *J. Solid State Chem.* **3,** 323 (1971).
42. H. Takizawa and H. Steinfink, *J. Solid State Chem.* **121,** 133 (1996), doi: 10.1006/jssc.1996.0019.
43. P. D. Battle, C. M. Davidson, T. C. Gibb, and J. F. Vente, *J. Mater. Chem.* **6,** 1187 (1996).
44. R. V. Shpanchenko, A. M. Abakumov, E. V. Antipov, L. Nistor, G. Van Tendeloo, and S. Amelinckx, *J. Solid State Chem.* **118,** 180 (1995), doi:10.1006/jssc.1995.1329.
45. R. D. Shannon, *Acta Crystallogr. A* **32,** 751 (1976).
46. I. D. Brown, "Structure and Bonding in Crystals" (M. O'Keeffe and A. Navrotsky, Eds.), Vol. 1. Academic Press, New York, 1981.
47. N. E. Brese and M. O'Keeffe, *Acta Crystallogr. B* **47,** 192 (1991).
48. M. O'Keeffe and N. E. Brese, *J. Am. Chem. Soc.* **113,** 3226 (1991).